Composite Fermi Liquid at Zero Magnetic Field in Twisted math xmlns="http://www.w3.org/1998/Math/MathML" display="inline">mrow>msub>mrow>mi>MoTe/mi>/mrow>mrow>mn>2/mn>/mrow>/msub>/mrow>/math>

Junkai Dong, Jie Wang, Patrick J. Ledwith, Ashvin Vishwanath, and Daniel E. Parker

Phys. Rev. Lett. **131**, 136502 — Published 27 September 2023

DOI: 10.1103/PhysRevLett.131.136502

Composite Fermi Liquid at Zero Magnetic Field in Twisted $MoTe_2$

Junkai Dong,[1,*] Jie Wang,[1,2,†] Patrick J. Ledwith,[1,‡] Ashvin Vishwanath,[1,§] and Daniel E. Parker[1,¶]

[1]*Department of Physics, Harvard University, Cambridge, MA 02138, USA*
[2]*Center for Mathematical Sciences and Applications, Harvard University, Cambridge, MA 02138, USA*

The pursuit of exotic phases of matter outside of the extreme conditions of a quantizing magnetic field is a longstanding quest of solid state physics. Recent experiments have observed spontaneous valley polarization and fractional Chern insulators (FCIs) in zero magnetic field in twisted bilayers of $MoTe_2$, at partial filling of the topological valence band ($\nu = -2/3$ and $-3/5$). We study the topological valence band at *half* filling, using exact diagonalization and density matrix renormalization group calculations. We discover a composite Fermi liquid (CFL) phase even at zero magnetic field that covers a large portion of the phase diagram near twist angle $\sim 3.6^\circ$. The CFL is a non-Fermi liquid phase with metallic behavior despite the absence of Landau quasiparticles. We discuss experimental implications including the competition between the CFL and a Fermi liquid, which can be tuned with a displacement field. The topological valence band has excellent quantum geometry over a wide range of twist angles and a small bandwidth that is, remarkably, reduced by interactions. These key properties stablize the exotic zero field quantum Hall phases. Finally, we present an optical signature involving "extinguished" optical responses that detects Chern bands with ideal quantum geometry.

Strong interactions can lead to exotic phases of matter such as non-Fermi liquids. A remarkable example is the composite Fermi liquid (CFL) that occurs in a half or quarter filled lowest Landau level (LLL). The CFL is a non-Fermi liquid with an emergent Fermi sea composed of charge neutral "composite fermions" [1–4] and has anomalous responses to a wide variety of experimental probes [5–10]. The gapless CFL state has provided an elegant interpretation for various Abelian [1–4] and non-Abelian gapped topological phases [11].

This work proposes an alternative route to realize CFLs. Our proposal is based on twisted 2D transition metal dichalcogenides (TMD), a family of platforms that have realized a wealth of interesting phenomena [12–27], and generated much theoretical interest for their topological properties [28–41]. A recent experiment [26] provided strong evidence for zero field fractional Chern insulators (FCIs) [42–45] at fillings $\nu = -2/3$ and $-3/5$ in twisted bilayer $MoTe_2$ ($tMoTe_2$). The $\nu = -2/3$ FCI was separately found by Ref. [27]. These experiments were preceded by theoretical models of Chern bands in $tMoTe_2$ [29], as well as numerical works that found FCIs at partial fillings in $MoTe_2$ [46] and in WSe_2 [47, 48]. More recently, theoretical studies combining *ab-initio* lattice relaxation and exact diagonalization on $tMoTe_2$ [49, 50] have also obtained FCIs.

FCIs were previously reported at high magnetic fields [51] by partially filling Hofstadter bands [52] of a substrate-induced moiré potential in graphene. Shortly thereafter, with the discovery of correlated phenomena [53, 54] and spontaneous Chern insulators [55–57] in twisted bilayer graphene (TBG), FCIs in zero field were theoretically anticipated in magic-angle TBG [58–60]. Experimental observations of FCIs in this setting soon appeared [61], albeit in a small magnetic field that theory [62] found was needed to improve the bandwidth and quantum geometry. These barriers are strikingly absent in $tMoTe_2$, motivating us to go beyond zero field FCIs to an exotic gapless state — the CFL.

We will focus on the gapless CFL phase, which presents challenges [63–66] relative to the well-understood spectral and entanglement signatures present in gapped FCI phases [67–72]. Combining large scale exact diagonalization (ED) with density matrix renormalization group (DMRG) numerics, we find a broad CFL phase at experimentally realistic parameters of $tMoTe_2$. Furthermore, we present an explicit trial wavefunction that captures the essential features of the zero field CFL and its low energy spectrum. Finally, we discuss experimental signatures that distinguish the CFL from Fermi liquids, enabling experimental exploration.

Continuum model.—We consider a model [29] for the valence bands of a twisted TMD with gate-screened [73] Coulomb interactions

$$\hat{H} = -\hat{h} + \frac{1}{2A}\sum_{\boldsymbol{q}} V_{\boldsymbol{q}} : \hat{\rho}_{\boldsymbol{q}}\hat{\rho}_{-\boldsymbol{q}} :, \;\; V_q = \frac{2\pi\tanh(qd)}{\epsilon_r\epsilon_0 q}, \quad (1)$$

where $\hat{\rho}_{\boldsymbol{q}}$ is the density operator, A is the sample area, normal ordering is relative to filling $\nu = 0$, d is gate distance, and $\epsilon_r \approx 8-40$ is the dielectric constant [49]. Due to spin-valley locking [29], the low energy holes of the K (K') valley are locked to spin up (down). The total kinetic term is $h = h_K + h_{K'}$ with [29]

$$h_K = \begin{bmatrix} h^b(\boldsymbol{r}) + V/2 & T(\boldsymbol{r}) \\ T^\dagger(\boldsymbol{r}) & h^t(\boldsymbol{r}) - V/2 \end{bmatrix}, \quad (2)$$

where $h^\ell(\boldsymbol{r}) = -(\boldsymbol{p} - \hbar v_F \boldsymbol{K}^\ell)^2/2m^* + \Delta^\ell(\boldsymbol{r})$ and $h_{K'}$ is determined by time-reversal. Here the layer-diagonal terms include the quadratic monolayer TMD

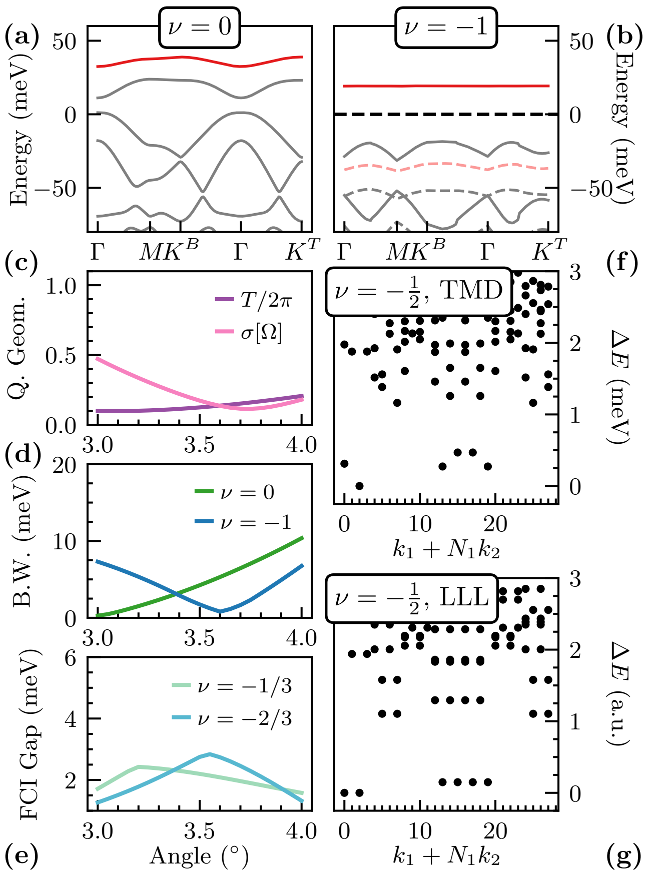

FIG. 1. The top valence band has favorable conditions for fractionalized topological phases. Bandstructure as seen from (a) charge neutrality and (b) from $\nu = -1$ computed from self-consistent Hartree-Fock. (c) Quantum geometry in terms of trace condition T and Berry curvature deviation $\sigma[\Omega]$. (d) Bare and SCHF bandwidths and (e) the many-body gap of FCIs at $\nu = -1/3$ and $\nu = -2/3$ as a function of twist angle. The FCI gaps are obtained from ED with $N_e = 8$ and 16 respectively. (f) and (g): ED spectrum for 14 particles at half filling for Coulomb interaction in lowest Landau level and screened Coulomb interaction in twisted $MoTe_2$, respectively. Parameters: $(\theta, \epsilon_r, d) = (3.7°, 15, 300\,Å)$ unless otherwise noted.

dispersion centered at rotated monolayer K-points $\boldsymbol{K}^{t/b}$, shifted by the displacement field V, and the moiré potentials $\Delta^{b/t}(\boldsymbol{r}) = 2v \sum_{j=1,3,5} \cos(\boldsymbol{b}_j \cdot \boldsymbol{r} \pm \psi)$. The off-diagonal terms are interlayer tunnelings $T(\boldsymbol{r}) = \omega\left(1 + e^{i\boldsymbol{b}_2\cdot\boldsymbol{r}} + e^{i\boldsymbol{b}_3\cdot\boldsymbol{r}}\right)$, where $\boldsymbol{b}_j$ are the reciprocal vectors obtained by counterclockwise $(j-1)\pi/3$ rotations of $\boldsymbol{b}_1 = (4\pi 3^{-1/2}\theta/a_0, 0)$. We focus on $tMoTe_2$, where recent first-principles calculations [49] (see also [29, 50]) found $(a_0, m^*, V, \psi, \omega) = (3.52\,Å, 0.6m_e, 20.8\,\text{meV}, -107.7°, -23.8\,\text{meV})$. We take $\theta = 3.7°$ throughout.

Flat Almost-Ideal Chern Band.—Fig. 1(a) shows the bandstructure for electrons h_K. The top moiré band has Chern number $C = 1$, due to the skyrmionic character of the layer spinor [29].

Recent experiments [26, 27] demonstrate that the many-body ground state is ferromagnetic (valley-polarized) in at least the range $-1.2 \lesssim \nu \lesssim -0.4$. The "parent state" for this regime is the correlated insulating state at $\nu = -1$. Fig. 1(b) shows its bandstructure within self-consistent Hartree-Fock (SCHF), which is strongly renormalized by interactions. Strikingly, the renormalized $C = 1$ band (red) becomes almost exactly flat, with bandwidth 1.6 meV at $\theta = 3.7°$. This *reduction* [74] in bandwidth from interaction effects is highly unusual [75].

The many-body physics of such flat bands is determined by the Bloch wavefunctions, often through their "quantum geometry". Recent theories [42, 58, 76–87] emphasize the role of Kähler geometry in FCI stability. We say that a band has "ideal quantum geometry" if the trace inequality $T = \int d^2\boldsymbol{k}\,(\mathrm{Tr}\, g_{\mathrm{FS}}(\boldsymbol{k}) - \Omega(\boldsymbol{k})) \geq 0$ is saturated [58, 79, 83, 88]; here g_{FS} is the Fubini-Study metric and Ω is the Berry curvature. Ideal bands are "vortexable" in the sense that $\hat{z}P = P\hat{z}P$ where P is the projector onto the band and $\hat{z} = \hat{x} + i\hat{y}$ [85, 89]. Vortexability enables the direct construction of Laughlin-like FQHE trial states that are exact many-body ground states for ideal bands with short-range interactions [85, 89, 90]. Fig. 1(c) shows T, the deviation from ideality, and $\sigma[\Omega]$, the standard deviation of Berry curvature. Both are small in $tMoTe_2$ for $3° \leq \theta \leq 4°$. The top valence band thus has the rare combination of excellent quantum geometry and negligible bandwidth that favors lattice realizations of exotic quantum Hall states at zero magnetic field.

The interacting physics of the flat band is modelled by projecting Eq. (1) via $-\hat{h} \to \sum_{\boldsymbol{k}} \epsilon(\boldsymbol{k}) \hat{c}^\dagger_{\boldsymbol{k}} \hat{c}_{\boldsymbol{k}}$ and $\hat{\rho}_{\boldsymbol{q}} \to \overline{\rho}_{\boldsymbol{q}} = \sum_{\boldsymbol{k}} \hat{c}^\dagger_{\boldsymbol{k}} \langle u_{\boldsymbol{k}} | u_{\boldsymbol{k}+\boldsymbol{q}} \rangle \hat{c}_{\boldsymbol{k}+\boldsymbol{q}}$ where $\epsilon(\boldsymbol{k})$ and $u_{\boldsymbol{k}}$ are the dispersion and periodic part of Bloch wavefunction. Fig. 1(d) shows the bare ($\nu = 0$) and renormalized ($\nu = -1$) bandwidths versus twist angle, minimized near 3° and 3.6°, respectively. Fig. 1(e) confirms that FCIs are stabilized at $\nu = -1/3, -2/3$ — in concord with previous results [46, 49, 50]. The mild angular dependence should make FCIs relatively robust to twist angle disorder. Notably the gap at $\nu = -2/3$ is largest where the bandwidth at $\nu = -1$ is smallest [91]. We therefore expect ∼3.6° to be optimal for FQH physics at half filling.

Composite Fermi liquid at $\nu = -1/2$.— We now go beyond gapped FCIs and examine the more exotic gapless CFL state [1, 11]. We focus on $\nu = -1/2$ but our conclusions also apply to $\nu = -3/4$ (data in SM [92]).

(i) Many body spectrum: Fig. 1(f, g) compares the spectra of twisted $MoTe_2$ and the lowest Landau level (LLL) at half filling with 14 electrons, showing a one-to-one correspondence at low energy. The LLL spectrum uses the same geometry as $tMoTe_2$ with Coulomb interactions. This one-to-one similarity holds at all system sizes $N_e = 8 - 14$. We thus conclude that the ground state of $\hat{H}$ at $\nu = -1/2$ is the same phase as the half-

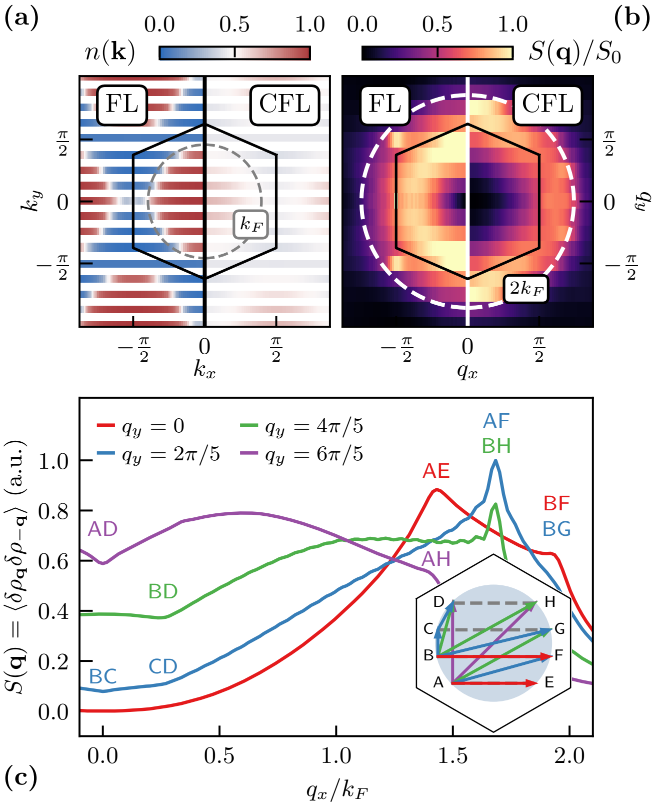

FIG. 2. Numerical identification of the composite Fermi liquid (CFL) from iDMRG. (a) Occupations $n(\boldsymbol{k})$ in the Brillouin zone at $L_y = 8$ for the Fermi liquid (FL, left side) versus the CFL (right side). (b) Connected structure factor $S(\boldsymbol{q}) = \langle \hat{\rho}_{\boldsymbol{q}} \hat{\rho}_{-\boldsymbol{q}} \rangle - \langle \hat{\rho}_{\boldsymbol{q}} \rangle \langle \hat{\rho}_{-\boldsymbol{q}} \rangle$ at $L_y = 8$. Characteristic features of a Fermi surface are visible for both the FL and CFL: near-vanishing weight outside $|\boldsymbol{q}| \approx 2k_F$, and peaks corresponding to momentum transfers inside that radius. (c) Cuts of $S(\boldsymbol{q})$ at constant q_y for $L_y = 5$ for the CFL. Each peak or inflection in $S(\boldsymbol{q})$ quantitatively matches scattering events across the almost-circular composite Fermi surface (Inset). Parameters match Fig. 1 with $\epsilon_r = 15$ (100) for the CFL (FL).

filled LLL with Coulomb interactions — the CFL. The ground state and low-energy excitations are at precisely the momenta expected for compact composite Fermi sea (CFS) configurations [93]. See SM for other system sizes, and detailed matching of degeneracies, momenta, and excitations to CFL expectations.

(ii) Absence of electron Fermi surface: A finite quasiparticle weight $Z > 0$ gives the jump in electron occupations $n(\boldsymbol{k})$ at the Fermi surface in a regular Fermi liquid (FL). As a non-Fermi liquid, composite fermions have vanishing Z, leading to the absence of Fermi surface occupation discontinuities.

To characterize the CFL, we employ large-scale iDMRG [94, 95] calculations with the TenPy library [96]. We use an infinite cylinder geometry with circumference $L_y = 5 - 10$, corresponding to L_y evenly spaced horizontal wires through the Brillouin zone (Fig. 2(c) inset). We take a computational basis of hybrid Wannier orbitals [97–99], and use "MPO compression" [100, 101] to accurately capture gate-screened Coulomb interactions in the flat band. Under weak interactions ($\epsilon_r = 100$), we find the FL expected from band theory at $\nu = -1/2$, with an almost-circular Fermi surface centered at Γ (Fig. 2(a), left) with radius $k_F = (A_{\rm BZ}/2\pi)^{1/2}$. The SM shows electrons, holes, and particle-hole pairs are likely gapless [102], confirming the Fermi liquid.

Under realistic interactions ($\epsilon_r = 15$) with the same parameters, the ground state has quasi-uniform occupations $|n(\boldsymbol{k}) - \frac{1}{2}| < 0.17$ (Fig. 2(a), right). Because charge $Q_E = 1$ correlations are short-ranged, the state is inconsistent with an electronic Fermi liquid. However, the state has high entanglement and significant electrically-neutral correlations, consistent with the gapless density fluctuations expected from an emergent CFS. To reveal the "hidden" CFS, we turn to the structure factor.

(iii) Scattering across the composite Fermi sea: Fig. 2(b) contrasts the connected structure factor $S(\boldsymbol{q}) = \langle \hat{\rho}_{\boldsymbol{q}} \hat{\rho}_{-\boldsymbol{q}} \rangle - \langle \hat{\rho}_{\boldsymbol{q}} \rangle \langle \hat{\rho}_{-\boldsymbol{q}} \rangle$ between the FL and the CFL. Both nearly vanish when $|\boldsymbol{q}| > 2k_F$, strongly implying that there is a Fermi surface in the CFL phase whose constituent fermions aren't electrons. We then match the features of $S(\boldsymbol{q})$ to scattering events with different momentum transfers across the putative CFS in Fig. 2(c), e.g. $\hat{c}^\dagger_{\boldsymbol{k}=G} \hat{c}_{\boldsymbol{k}=B}$ scattering with $q_x \approx 1.94 k_F$. The *tour-de-force* work of Geraedts *et al* [63] showed such features are emblematic of the CFS arising from the half-filled LLL. As every feature in $S(\boldsymbol{q})$ corresponds to such a scattering (quantitative matching in SM), we conclude the state has an almost-circular [103] CFS composed of non-Landau quasiparticles. These two independent numerical methods establish a CFL state at $\nu = -1/2$ (see SM for $\nu = -3/4$).

Zero Field CFL Wavefunction.— Standard theories of composite fermions apply at $B > 0$, where emergent gauge flux cancels external magnetic flux. These cannot apply directly here at zero magnetic field. We therefore construct an explicit zero-field CFL wavefunction. To start, we approximate the geometry of the top $\mathrm{tMoTe_2}$ band as ideal. Such bands have the general "LLL-like" wavefunction [58, 83],

$$\psi_l(\boldsymbol{r}) = \phi(\boldsymbol{r})\zeta_l(\boldsymbol{r}) = f(z)e^{-K(\boldsymbol{r})}\zeta_l(\boldsymbol{r}), \tag{3}$$

where $f(z)$ is holomorphic and $\zeta_l(\boldsymbol{r})$ is an orbital-space spinor where $\sum_l |\zeta_l(\boldsymbol{r})|^2 = 1$. Here $\phi(\boldsymbol{r})$ is the wavefunction of a Dirac particle in an inhomogeneous, periodic, magnetic field $B(\boldsymbol{r}) = \nabla^2 \mathrm{Re} K(\boldsymbol{r})$ with one flux per unit cell [58, 104, 105]. While ψ is symmetric under ordinary translations, $\phi(\boldsymbol{r})$ and $\zeta_l(\boldsymbol{r})$ are symmetric under *magnetic* translations, with opposite magnetic twists [106], giving a gauge redundancy $\phi(\boldsymbol{r}) \to e^{+i\lambda(\boldsymbol{r})}\phi(\boldsymbol{r}), \zeta_l(\boldsymbol{r}) \to e^{-i\lambda(\boldsymbol{r})}\zeta_l(\boldsymbol{r})$. The form Eq.(3) implies that *all* many-body wavefunctions within the band of interest have the form

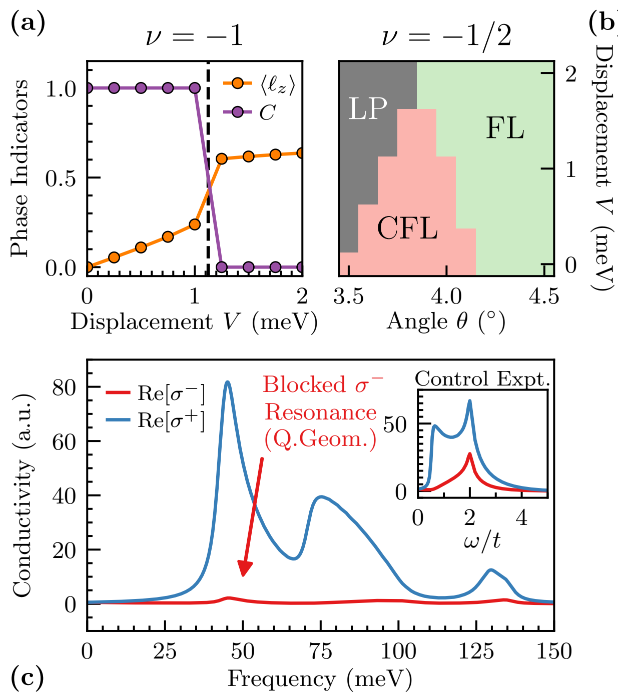

FIG. 3. Many-body phase diagrams and optical responses. (a) Phase diagram at $\nu=-1$ with $\theta=3.7^\circ$ showing a transition from $C=1$ layer-unpolarized state to a $C=0$ layer polarized state. (b) Phase diagram of the topological regime at $\nu=-1/2$: The CFL phase is shown in red, whereas the green region corresponds to the FL phase. Here 'LP' indicates a layer polarization instability determined from $\nu=-1$ SCHF. (c) Direct optical probe of almost-ideal quantum geometry via an "extinguished" valence-valence optical responses in σ^-, Inset: the Haldane model at $(t,t_2)=(1,0.05)$ has non-ideal geometry. Parameters match Fig. 1.

$\Psi=\Psi_\phi\prod_i\zeta_{l_i}(\boldsymbol{r}_i)$, where Ψ_ϕ is a wavefunction of flux-feeling particles; in the SM we interpret this fractionalization in terms of a new type of Chern band parton theory [107, 108]; see also [109–114]. For example, we may use Read & Rezayi's LLL ansatz for the CFL [115] to obtain:

$$\Psi(\{\boldsymbol{r}_i\})=\mathcal{P}\det_{ij}\psi^{\rm CF}_{\boldsymbol{k}_i}(\boldsymbol{r}_j)\prod_{i<j}(z_i-z_j)^2\prod_i e^{-K(\boldsymbol{r}_i)}\zeta_{l_i}(\boldsymbol{r}_i). \tag{4}$$

Here $\mathcal{P}=\prod_i P_i$ is the many-body projector to the top band, and $\psi^{\rm CF}_{\boldsymbol{k}_i}$ fill a Fermi sea [116].

Experimental Signatures.— We conclude with experimental implications of the quantum geometry and CFL phase. Fig. 3(a,b) show phase diagrams of $tMoTe_2$. At $\nu=-1$, SCHF finds the $|C|=1$ phase transitions to an valley and layer polarized phase at large V. At $\nu=-1/2$, we find a broad CFL phase centered around 3.8° that competes with layer polarized phases and $C=1$ Fermi liquids at larger V. The layer polarized region is estimated from SCHF at $\nu=-1$, where an interaction-driven layer-polarized state is more favorable. The phase diagram at $\nu=-3/4$ is similar (see SM), except the CFL is more sensitive to displacement field.

The almost ideal quantum geometry manifests optically. If a band with projector P is vortexable, then $\hat{z}P=P\hat{z}P$ implies the velocity operator $\hat{v}^\pm=-i[\hat{x}\pm i\hat{y},\hat{H}]$ must obey $(I-P)\hat{v}^+P=0$, i.e. left-circularly polarized transitions are "extinguished". This gives perfect circular dichroism:

$$\frac{\sigma^+-\sigma^-}{\sigma^++\sigma^-}=1;\ \sigma^\pm(\omega)=\frac{ie^2}{\hbar}\sum_{\boldsymbol{k},a\neq b=0}\frac{f_{ab}}{\epsilon_{ab}}\frac{\left|\langle\psi_{\boldsymbol{k}a}|\hat{v}^\pm|\psi_{\boldsymbol{k}b}\rangle\right|^2}{\omega-\epsilon_{ab}}. \tag{5}$$

Here $\epsilon_{ab}=\epsilon_a-\epsilon_b$ are energy differences and $f_{ab}=f(\epsilon_a)-f(\epsilon_b)$ are Fermi factors. Fig. 3(c) shows $\sigma^\pm$ for $tMoTe_2$ at $\nu=-1$. As the $C=+1$ band is nearly vortexable, transitions from the second and third valence bands to the empty top valence band nearly vanish, giving nearly-perfect circular dichroism >0.9 at resonance. The inset shows a control experiment: the Haldane model has Chern bands $C=\pm1$ but not ideal geometry; σ^- is not extinguished there.

Finally, we discuss direct experimental probes of the zero-field CFL. While the CFL and the FL are both compressible and metallic, they differ in that the CFL's excitations have vanishing overlap with the electron in the limit of low energies, and CFs themselves are best thought of as (doubled) *vortices* in the electronic fluid [3, 4, 117–119]. This observation leads to a number of striking physical responses that differ strongly from Fermi liquids. These include (i) a "pseudogap" in the tunneling density of states $A(\omega)\propto e^{-\omega_0/\omega}$ [120] as a function of bias ω, which has been observed between two CFLs with a tunnel barrier [5]; (ii) distinct DC conductivity in the clean limit: $\sigma_{xx}\to0$ in a CFL in the absence of disorder $k_Fl\to\infty$, whereas in the FL, even in a Chern band, σ_{xx} diverges [121]; (iii) strong violation of the Wiedemann-Franz law [118, 119] which compares heat and charge transport; (iv) quantum oscillations with doping, that CFs feel a magnetic field $\propto(\nu-1/2)$ and can fill Landau levels, leading to Jain-like [1] FCIs when fully developed, which can further be probed using geometric resonance with a one-dimensional periodic grating [3, 6, 7]; (v) vanishing thermoelectric conductance $\alpha_{xx}=j_x/(-\partial_xT)$ due to approximate emergent particle-hole symmetry [122, 123]; (vi) surface acoustic wave attenuation, a contactless probe that measures $\sigma_{xx}(\boldsymbol{q})\propto|\boldsymbol{q}|$ in the CFL [3], as opposed to $\sigma_{xx}\propto|\boldsymbol{q}|^{-1}$ in a clean FL [8].

Finally we highlight properties of zero field CFLs that transcend LLL physics. First, the Chern bands of $MoTe_2$ have one effective magnetic flux quantum per moiré unit cell, translating to 160 T at 3.7°. This vastly exceeds laboratory magnetic fields, leading to enhanced energy scales. The lack of *real* quantizing magnetic fields, however, opens up the possibility of employing zero field experimental probes such as high resolution angle-resolved photoemission spectroscopy (ARPES). Furthermore, the exponentially suppressed tunneling density of states of the CFL could be probed through tunneling from a proximate Fermi liquid state, or via spatial variation of the twist angle, which can be used to create a CFL-FL interface within the same sample. Our work does not rule out the possibility of a continuous quantum phase transition, driven by displacement field, between the CFL and FL [113], which could be studied experimentally. Since the effective magnetic field of the TMD originates from spontaneous breaking of time reversal symmetry through valley polarization, rather than external magnetic field, domains between opposite valley polarizations and hence between time-reversal-related CFLs are expected. Transport properties across such a domain wall would interrogate composite fermions in an entirely new regime, and potentially shed light on their proposed Dirac character [4, 117, 119]. Finally, we note that moiré phonons occur on the same scale as the effective magnetic length in this system; their interplay with CFL physics is unclear at present and worthy of future study.

We thank Junyeong Ahn, Ilya Esterlis, Eslam Khalaf, Jiaqi Cai, Richard Averitt, Darius Torchinsky, and especially Bertrand Halperin for helpful discussions. We acknowledge Michael Zaletel, Tomohiro Soejima, and Johannes Hauschild for ongoing and related collaborations. We sincerely thank Taige Wang for alerting us to the importance of layer polarization after our paper was announced on arXiv. Shortly after this manuscript was posted, [124, 125] appeared, which overlaps with parts of this work. Additionally, Ref. [126] overlaps with the optical responses discussed here. Subsequent to our work, transport experiments [127] on twisted $MoTe_2$ were performed and the results are consistent with our findings. A.V. is supported by the Simons Collaboration on Ultra-Quantum Matter, which is a grant from the Simons Foundation (651440, A.V.) and by the Center for Advancement of Topological Semimetals, an Energy Frontier Research Center funded by the US Department of Energy Office of Science, Office of Basic Energy Sciences, through the Ames Laboratory under contract No. DE-AC02-07CH11358. This research is funded in part by the Gordon and Betty Moore Foundation's EPiQS Initiative, Grant GBMF8683 to D.E.P.

* junkaidong@g.harvard.edu
† jiewang@fas.harvard.edu
‡ pledwith@g.harvard.edu
§ avishwanath@g.harvard.edu
¶ daniel_parker@fas.harvard.edu

[1] J. K. Jain. Composite-fermion approach for the fractional quantum hall effect. *Phys. Rev. Lett.*, 63:199–202, Jul 1989.

[2] Ana Lopez and Eduardo Fradkin. Fractional quantum hall effect and chern-simons gauge theories. *Phys. Rev. B*, 44:5246–5262, Sep 1991.

[3] B. I. Halperin, Patrick A. Lee, and Nicholas Read. Theory of the half-filled landau level. *Phys. Rev. B*, 47:7312–7343, Mar 1993.

[4] Dam Thanh Son. Is the composite fermion a dirac particle? *Phys. Rev. X*, 5:031027, Sep 2015.

[5] J. P. Eisenstein, L. N. Pfeiffer, and K. W. West. Coulomb barrier to tunneling between parallel two-dimensional electron systems. *Phys. Rev. Lett.*, 69:3804–3807, Dec 1992.

[6] R. L. Willett, R. R. Ruel, K. W. West, and L. N. Pfeiffer. Experimental demonstration of a fermi surface at one-half filling of the lowest landau level. *Phys. Rev. Lett.*, 71:3846–3849, Dec 1993.

[7] W. Kang, H. L. Stormer, L. N. Pfeiffer, K. W. Baldwin, and K. W. West. How real are composite fermions? *Phys. Rev. Lett.*, 71:3850–3853, Dec 1993.

[8] R. L. Willett, R. R. Ruel, M. A. Paalanen, K. W. West, and L. N. Pfeiffer. Enhanced finite-wave-vector conductivity at multiple even-denominator filling factors in two-dimensional electron systems. *Phys. Rev. B*, 47:7344–7347, Mar 1993.

[9] V. J. Goldman, B. Su, and J. K. Jain. Detection of composite fermions by magnetic focusing. *Phys. Rev. Lett.*, 72:2065–2068, Mar 1994.

[10] J. H. Smet, D. Weiss, R. H. Blick, G. Lütjering, K. von Klitzing, R. Fleischmann, R. Ketzmerick, T. Geisel, and G. Weimann. Magnetic focusing of composite fermions through arrays of cavities. *Phys. Rev. Lett.*, 77:2272–2275, Sep 1996.

[11] N. Read and Dmitry Green. Paired states of fermions in two dimensions with breaking of parity and time-reversal symmetries and the fractional quantum hall effect. *Phys. Rev. B*, 61:10267–10297, Apr 2000.

[12] Yanhao Tang, Lizhong Li, Tingxin Li, Yang Xu, Song Liu, Katayun Barmak, Kenji Watanabe, Takashi Taniguchi, Allan H. MacDonald, Jie Shan, and Kin Fai Mak. Simulation of hubbard model physics in wse2/ws2 moirésuperlattices. *Nature*, 579(7799):353–358, 2020.

[13] Yang Xu, Kaifei Kang, Kenji Watanabe, Takashi Taniguchi, Kin Fai Mak, and Jie Shan. A tunable bilayer hubbard model in twisted WSe2. *Nature Nanotechnology*, 17(9):934–939, aug 2022.

[14] L. Wang, E.-M. Shih, A. Ghiotto, D. A. Rhodes L. Xian, C. Tan, M. Claassen, D. M. Kennes, Y. Bai, B. Kim, K. Watanabe, T. Taniguchi, X. Zhu, J. Hone, A. Rubio, A. N. Pasupathy, and C. R. Dean. Correlated electronic phases in twisted bilayer transition metal dichalcogenides. *Nature Materials*, 19:861–866, 2020.

[15] Yang Xu, Song Liu, Daniel A. Rhodes, Kenji Watanabe, Takashi Taniguchi, James Hone, Veit Elser, Kin Fai Mak, and Jie Shan. Correlated insulating states at fractional fillings of moirésuperlattices. *Nature*, 587(7833):214–218, 2020.

[16] Xiong Huang, Tianmeng Wang, Shengnan Miao, Chong Wang, Zhipeng Li, Zhen Lian, Takashi Taniguchi, Kenji Watanabe, Satoshi Okamoto, Di Xiao, Su-Fei Shi, and Yong-Tao Cui. Correlated insulating states at fractional fillings of the WS2/WSe2 moiré lattice. *Nature Physics*, 17(6):715–719, feb 2021.

[17] Emma C. Regan, Danqing Wang, Chenhao Jin, M. Iqbal Bakti Utama, Beini Gao, Xin Wei, Sihan Zhao, Wenyu Zhao, Zuocheng Zhang, Kentaro Yumigeta, Mark Blei, Johan D. Carlström, Kenji Watanabe, Takashi

Taniguchi, Sefaattin Tongay, Michael Crommie, Alex Zettl, and Feng Wang. Mott and generalized wigner crystal states in wse2/ws2 moirésuperlattices. *Nature*, 579(7799):359–363, 2020.

[18] Tingxin Li, Shengwei Jiang, Lizhong Li, Yang Zhang, Kaifei Kang, Jiacheng Zhu, Kenji Watanabe, Takashi Taniguchi, Debanjan Chowdhury, Liang Fu, Jie Shan, and Kin Fai Mak. Continuous mott transition in semiconductor moiré superlattices. *Nature*, 597(7876):350–354, sep 2021.

[19] Augusto Ghiotto, En-Min Shih, Giancarlo S. S. G. Pereira, Daniel A. Rhodes, Bumho Kim, Jiawei Zang, Andrew J. Millis, Kenji Watanabe, Takashi Taniguchi, James C. Hone, Lei Wang, Cory R. Dean, and Abhay N. Pasupathy. Quantum criticality in twisted transition metal dichalcogenides. *Nature*, 597(7876):345–349, sep 2021.

[20] Tingxin Li, Shengwei Jiang, Bowen Shen, Yang Zhang, Lizhong Li, Zui Tao, Trithep Devakul, Kenji Watanabe, Takashi Taniguchi, Liang Fu, Jie Shan, and Kin Fai Mak. Quantum anomalous hall effect from intertwined moiré bands. *Nature*, 600(7890):641–646, dec 2021.

[21] Wenjin Zhao, Kaifei Kang, Lizhong Li, Charles Tschirhart, Evgeny Redekop, Kenji Watanabe, Takashi Taniguchi, Andrea Young, Jie Shan, and Kin Fai Mak. Realization of the haldane chern insulator in a moiré lattice, 2022.

[22] Zui Tao, Bowen Shen, Shengwei Jiang, Tingxin Li, Lizhong Li, Liguo Ma, Wenjin Zhao, Jenny Hu, Kateryna Pistunova, Kenji Watanabe, Takashi Taniguchi, Tony F. Heinz, Kin Fai Mak, and Jie Shan. Valley-coherent quantum anomalous hall state in ab-stacked mote2/wse2 bilayers, 2022.

[23] Benjamin A. Foutty, Jiachen Yu, Trithep Devakul, Carlos R. Kometter, Yang Zhang, Kenji Watanabe, Takashi Taniguchi, Liang Fu, and Benjamin E. Feldman. Tunable spin and valley excitations of correlated insulators in *upGamma*-valley moiré bands. *Nature Materials*, apr 2023.

[24] Benjamin A. Foutty, Carlos R. Kometter, Trithep Devakul, Aidan P. Reddy, Kenji Watanabe, Takashi Taniguchi, Liang Fu, and Benjamin E. Feldman. Mapping twist-tuned multi-band topology in bilayer wse_2, 2023.

[25] Eric Anderson, Feng-Ren Fan, Jiaqi Cai, William Holtzmann, Takashi Taniguchi, Kenji Watanabe, Di Xiao, Wang Yao, and Xiaodong Xu. Programming correlated magnetic states via gate controlled moiré geometry, 2023.

[26] Jiaqi Cai, Eric Anderson, Chong Wang, Xiaowei Zhang, Xiaoyu Liu, William Holtzmann, Yinong Zhang, Fengren Fan, Takashi Taniguchi, Kenji Watanabe, Ying Ran, Ting Cao, Liang Fu, Di Xiao, Wang Yao, and Xiaodong Xu. Signatures of Fractional Quantum Anomalous Hall States in Twisted MoTe2. *Nature*, pages 1–3, June 2023. Publisher: Nature Publishing Group.

[27] Yihang Zeng, Zhengchao Xia, Kaifei Kang, Jiacheng Zhu, Patrick Knüppel, Chirag Vaswani, Kenji Watanabe, Takashi Taniguchi, Kin Fai Mak, and Jie Shan. Thermodynamic evidence of fractional Chern insulator in moiré MoTe2. *Nature*, pages 1–2, July 2023. Publisher: Nature Publishing Group.

[28] Fengcheng Wu, Timothy Lovorn, Emanuel Tutuc, and A. H. MacDonald. Hubbard model physics in transition metal dichalcogenide moiré bands. *Phys. Rev. Lett.*, 121:026402, Jul 2018.

[29] Fengcheng Wu, Timothy Lovorn, Emanuel Tutuc, Ivar Martin, and A. H. MacDonald. Topological insulators in twisted transition metal dichalcogenide homobilayers. *Phys. Rev. Lett.*, 122:086402, Feb 2019.

[30] Hongyi Yu, Mingxing Chen, and Wang Yao. Giant magnetic field from moiré induced berry phase in homobilayer semiconductors. *National Science Review*, 7(1):12–20, aug 2019.

[31] Dawei Zhai and Wang Yao. Theory of tunable flux lattices in the homobilayer moiré of twisted and uniformly strained transition metal dichalcogenides. *Phys. Rev. Mater.*, 4:094002, Sep 2020.

[32] Hao Tang, Stephen Carr, and Efthimios Kaxiras. Geometric origins of topological insulation in twisted layered semiconductors. *Physical Review B*, 104(15), oct 2021.

[33] Trithep Devakul, Valentin Crépel, Yang Zhang, and Liang Fu. Magic in twisted transition metal dichalcogenide bilayers. *Nature Communications*, 12(1), nov 2021.

[34] Yang Zhang, Trithep Devakul, and Liang Fu. Spin-textured chern bands in AB-stacked transition metal dichalcogenide bilayers. *Proceedings of the National Academy of Sciences*, 118(36), sep 2021.

[35] Ya-Hui Zhang, D. N. Sheng, and Ashvin Vishwanath. SU(4) chiral spin liquid, exciton supersolid, and electric detection in moiré bilayers. *Physical Review Letters*, 127(24), dec 2021.

[36] Jiawei Zang, Jie Wang, Jennifer Cano, and Andrew J. Millis. Hartree-fock study of the moiré hubbard model for twisted bilayer transition metal dichalcogenides. *Phys. Rev. B*, 104:075150, Aug 2021.

[37] Jie Wang, Jiawei Zang, Jennifer Cano, and Andrew J. Millis. Staggered pseudo magnetic field in twisted transition metal dichalcogenides: Physical origin and experimental consequences, 2021.

[38] Jiawei Zang, Jie Wang, Jennifer Cano, Antoine Georges, and Andrew J. Millis. Dynamical mean-field theory of moiré bilayer transition metal dichalcogenides: Phase diagram, resistivity, and quantum criticality. *Phys. Rev. X*, 12:021064, Jun 2022.

[39] Haining Pan, Fengcheng Wu, and Sankar Das Sarma. Band topology, hubbard model, heisenberg model, and dzyaloshinskii-moriya interaction in twisted bilayer wse_2. *Phys. Rev. Res.*, 2:033087, Jul 2020.

[40] Ahmed Abouelkomsan, Emil J. Bergholtz, and Shubhayu Chatterjee. Multiferroicity and topology in twisted transition metal dichalcogenides, 2022.

[41] Valentin Crépel, Nicolas Regnault, and Raquel Queiroz. The chiral limits of moiré semiconductors: origin of flat bands and topology in twisted transition metal dichalcogenides homobilayers, 2023.

[42] Siddharth A. Parameswaran, Rahul Roy, and Shivaji L. Sondhi. Fractional quantum hall physics in topological flat bands. *Comptes Rendus Physique*, 14(9-10):816–839, nov 2013.

[43] Titus Neupert, Claudio Chamon, Thomas Iadecola, Luiz H Santos, and Christopher Mudry. Fractional (chern and topological) insulators. *Physica Scripta*, T164:014005, aug 2015.

[44] EMIL J. BERGHOLTZ and ZHAO LIU. Topological flat band models and fractional chern insulators. *Inter-*

national Journal of Modern Physics B, 27(24):1330017, 2013.

[45] Zhao Liu and Emil J. Bergholtz. Recent developments in fractional chern insulators. In *Reference Module in Materials Science and Materials Engineering*. Elsevier, 2023.

[46] Heqiu Li, Umesh Kumar, Kai Sun, and Shi-Zeng Lin. Spontaneous fractional chern insulators in transition metal dichalcogenide moiré superlattices. *Phys. Rev. Research*, 3:L032070, Sep 2021.

[47] Valentin Crépel and Liang Fu. Anomalous hall metal and fractional chern insulator in twisted transition metal dichalcogenides. *Phys. Rev. B*, 107:L201109, May 2023.

[48] Nicolás Morales-Durán, Jie Wang, Gabriel R. Schleder, Mattia Angeli, Ziyan Zhu, Efthimios Kaxiras, Cécile Repellin, and Jennifer Cano. Pressure–enhanced fractional Chern insulators in moiré transition metal dichalcogenides along a magic line. *arXiv e-prints*, page arXiv:2304.06669, April 2023.

[49] Chong Wang, Xiao-Wei Zhang, Xiaoyu Liu, Yuchi He, Xiaodong Xu, Ying Ran, Ting Cao, and Di Xiao. Fractional Chern Insulator in Twisted Bilayer $MoTe_2$. *arXiv e-prints*, page arXiv:2304.11864, April 2023.

[50] Aidan P. Reddy, Faisal F. Alsallom, Yang Zhang, Trithep Devakul, and Liang Fu. Fractional quantum anomalous Hall states in twisted bilayer $MoTe_2$ and WSe_2. *arXiv e-prints*, page arXiv:2304.12261, April 2023.

[51] Eric M. Spanton, Alexander A. Zibrov, Haoxin Zhou, Takashi Taniguchi, Kenji Watanabe, Michael P. Zaletel, and Andrea F. Young. Observation of fractional chern insulators in a van der waals heterostructure. *Science*, 360(6384):62–66, apr 2018.

[52] A. Kol and N. Read. Fractional quantum hall effect in a periodic potential. *Phys. Rev. B*, 48:8890–8898, Sep 1993.

[53] Yuan Cao, Valla Fatemi, Ahmet Demir, Shiang Fang, Spencer L. Tomarken, Jason Y. Luo, Javier D. Sanchez-Yamagishi, Kenji Watanabe, Takashi Taniguchi, Efthimios Kaxiras, Ray C. Ashoori, and Pablo Jarillo-Herrero. Correlated insulator behaviour at half-filling in magic-angle graphene superlattices. *Nature*, 556(7699):80–84, 2018.

[54] Yuan Cao, Valla Fatemi, Shiang Fang, Kenji Watanabe, Takashi Taniguchi, Efthimios Kaxiras, and Pablo Jarillo-Herrero. Unconventional superconductivity in magic-angle graphene superlattices. *Nature*, 556(7699):43–50, 2018.

[55] Ya-Hui Zhang, Dan Mao, Yuan Cao, Pablo Jarillo-Herrero, and T. Senthil. Nearly flat chern bands in moiré superlattices. *Phys. Rev. B*, 99:075127, Feb 2019.

[56] Aaron L. Sharpe, Eli J. Fox, Arthur W. Barnard, Joe Finney, Kenji Watanabe, Takashi Taniguchi, M. A. Kastner, and David Goldhaber-Gordon. Emergent ferromagnetism near three-quarters filling in twisted bilayer graphene. *Science*, 365(6453):605–608, 2019.

[57] M. Serlin, C. L. Tschirhart, H. Polshyn, Y. Zhang, J. Zhu, K. Watanabe, T. Taniguchi, L. Balents, and A. F. Young. Intrinsic quantized anomalous hall effect in a moiré heterostructure. *Science*, 367(6480):900–903, 2020.

[58] Patrick J. Ledwith, Grigory Tarnopolsky, Eslam Khalaf, and Ashvin Vishwanath. Fractional chern insulator states in twisted bilayer graphene: An analytical approach. *Phys. Rev. Research*, 2:023237, May 2020.

[59] Ahmed Abouelkomsan, Kang Yang, and Emil J. Bergholtz. Quantum metric induced phases in moiré materials. *Phys. Rev. Res.*, 5:L012015, Feb 2023.

[60] Cécile Repellin and T. Senthil. Chern bands of twisted bilayer graphene: Fractional chern insulators and spin phase transition. *Phys. Rev. Research*, 2:023238, May 2020.

[61] Yonglong Xie, Andrew T. Pierce, Jeong Min Park, Daniel E. Parker, Eslam Khalaf, Patrick Ledwith, Yuan Cao, Seung Hwan Lee, Shaowen Chen, Patrick R. Forrester, Kenji Watanabe, Takashi Taniguchi, Ashvin Vishwanath, Pablo Jarillo-Herrero, and Amir Yacoby. Fractional chern insulators in magic-angle twisted bilayer graphene. *Nature*, 600(7889):439–443, 2021.

[62] Daniel Parker, Patrick Ledwith, Eslam Khalaf, Tomohiro Soejima, Johannes Hauschild, Yonglong Xie, Andrew Pierce, Michael P Zaletel, Amir Yacoby, and Ashvin Vishwanath. Field-tuned and zero-field fractional chern insulators in magic angle graphene. *arXiv preprint arXiv:2112.13837*, 2021.

[63] Scott D. Geraedts, Michael P. Zaletel, Roger S. K. Mong, Max A. Metlitski, Ashvin Vishwanath, and Olexei I. Motrunich. The half-filled landau level: The case for dirac composite fermions. *Science*, 352(6282):197–201, 2016.

[64] Matteo Ippoliti, Scott D. Geraedts, and R. N. Bhatt. Numerical study of anisotropy in a composite fermi liquid. *Phys. Rev. B*, 95:201104, May 2017.

[65] Matteo Ippoliti, Scott D. Geraedts, and R. N. Bhatt. Connection between fermi contours of zero-field electrons and $\nu = \frac{1}{2}$ composite fermions in two-dimensional systems. *Phys. Rev. B*, 96:045145, Jul 2017.

[66] Matteo Ippoliti, Scott D. Geraedts, and R. N. Bhatt. Composite fermions in bands with n-fold rotational symmetry. *Phys. Rev. B*, 96:115151, Sep 2017.

[67] Kai Sun, Zhengcheng Gu, Hosho Katsura, and S. Das Sarma. Nearly flatbands with nontrivial topology. *Phys. Rev. Lett.*, 106:236803, Jun 2011.

[68] D. N. Sheng, Zheng-Cheng Gu, Kai Sun, and L. Sheng. Fractional quantum hall effect in the absence of landau levels. *Nature Communications*, 2(1):389, 2011.

[69] Titus Neupert, Luiz Santos, Claudio Chamon, and Christopher Mudry. Fractional quantum hall states at zero magnetic field. *Phys. Rev. Lett.*, 106:236804, Jun 2011.

[70] Yi-Fei Wang, Zheng-Cheng Gu, Chang-De Gong, and D. N. Sheng. Fractional quantum hall effect of hard-core bosons in topological flat bands. *Phys. Rev. Lett.*, 107:146803, Sep 2011.

[71] Evelyn Tang, Jia-Wei Mei, and Xiao-Gang Wen. High-temperature fractional quantum hall states. *Phys. Rev. Lett.*, 106:236802, Jun 2011.

[72] N. Regnault and B. Andrei Bernevig. Fractional chern insulator. *Phys. Rev. X*, 1:021014, Dec 2011.

[73] Nick Bultinck, Shubhayu Chatterjee, and Michael P. Zaletel. Mechanism for anomalous hall ferromagnetism in twisted bilayer graphene. *Phys. Rev. Lett.*, 124:166601, Apr 2020.

[74] Adolfo G. Grushin, Titus Neupert, Claudio Chamon, and Christopher Mudry. Enhancing the stability of a fractional Chern insulator against competing phases. *Physical Review B*, 86(20):205125, November 2012.

[75] For example, in twisted bilayer graphene the single peak of charge density at AA sites gives a sharp Hartree peak, dramatically increasing the total bandwidth at fillings with a single active band [128]. In contrast, spin-valley locking in TMDs naturally isolates a single Chern band. Here charge density is doubly-peaked, so the interaction-generated dispersion is mild [129] — and almost perfectly cancels against the non-interacting dispersion. See also [44, 59, 130, 131].
[76] Rahul Roy. Band geometry of fractional topological insulators. *Phys. Rev. B*, 90:165139, Oct 2014.
[77] T. S. Jackson, Gunnar Möller, and Rahul Roy. Geometric stability of topological lattice phases. *Nature Communications*, 6(1):8629, 2015.
[78] Martin Claassen, Ching Hua Lee, Ronny Thomale, Xiao-Liang Qi, and Thomas P. Devereaux. Position-momentum duality and fractional quantum hall effect in chern insulators. *Phys. Rev. Lett.*, 114:236802, Jun 2015.
[79] Grigory Tarnopolsky, Alex Jura Kruchkov, and Ashvin Vishwanath. Origin of magic angles in twisted bilayer graphene. *Phys. Rev. Lett.*, 122:106405, Mar 2019.
[80] Tomoki Ozawa and Bruno Mera. Relations between topology and the quantum metric for chern insulators. *Phys. Rev. B*, 104:045103, Jul 2021.
[81] Bruno Mera and Tomoki Ozawa. Kähler geometry and chern insulators: Relations between topology and the quantum metric. *Phys. Rev. B*, 104:045104, Jul 2021.
[82] Bruno Mera and Tomoki Ozawa. Engineering geometrically flat chern bands with fubini-study kähler structure. *Phys. Rev. B*, 104:115160, Sep 2021.
[83] Jie Wang, Jennifer Cano, Andrew J. Millis, Zhao Liu, and Bo Yang. Exact landau level description of geometry and interaction in a flatband. *Phys. Rev. Lett.*, 127:246403, Dec 2021.
[84] Jie Wang and Zhao Liu. Hierarchy of ideal flatbands in chiral twisted multilayer graphene models. *Phys. Rev. Lett.*, 128:176403, Apr 2022.
[85] Patrick J. Ledwith, Ashvin Vishwanath, and Daniel E. Parker. Vortexability: A Unifying Criterion for Ideal Fractional Chern Insulators. *arXiv e-prints*, page arXiv:2209.15023, September 2022.
[86] Jie Wang, Semyon Klevtsov, and Zhao Liu. Origin of model fractional chern insulators in all topological ideal flatbands: Explicit color-entangled wave function and exact density algebra. *Phys. Rev. Res.*, 5:023167, Jun 2023.
[87] Junkai Dong, Patrick J. Ledwith, Eslam Khalaf, Jong Yeon Lee, and Ashvin Vishwanath. Many-body ground states from decomposition of ideal higher chern bands: Applications to chirally twisted graphene multilayers. *Phys. Rev. Res.*, 5:023166, Jun 2023.
[88] Daniel Varjas, Ahmed Abouelkomsan, Kang Yang, and Emil J. Bergholtz. Topological lattice models with constant Berry curvature. *SciPost Phys.*, 12:118, 2022.
[89] Patrick J. Ledwith, Ashvin Vishwanath, and Eslam Khalaf. Family of ideal chern flatbands with arbitrary chern number in chiral twisted graphene multilayers. *Phys. Rev. Lett.*, 128:176404, Apr 2022.
[90] S. A. Trugman and S. Kivelson. Exact results for the fractional quantum hall effect with general interactions. *Phys. Rev. B*, 31:5280–5284, Apr 1985.
[91] The gaps computed here correspond to the collective neutral excitations. To get the activation gap of charged particles, one should generally consider $\Delta E = (E_{N+1} + E_{N-1} - E_N)/2$, where E_N is the ground state energy of N electrons.
[92] See Supplemental Material [url] for a detailed description of the continuum model, a brief introduction to quantum geometry, a derivation of vortexability induced perfect circular dichroism, a parton theory for the zero field composite Fermi liquid in Chern bands, a discussion of interaction driven layer polarization physics, details and discussions on exact diagonalization numerics, details and discussions on density matrix renormalization group numerics, and more experimental signatures, which includes Refs. [128, 132–148].
[93] Scott D. Geraedts, Jie Wang, E. H. Rezayi, and F. D. M. Haldane. Berry phase and model wave function in the half-filled landau level. *Phys. Rev. Lett.*, 121:147202, Oct 2018.
[94] Steven R White. Density matrix formulation for quantum renormalization groups. *Physical review letters*, 69(19):2863, 1992.
[95] Ulrich Schollwöck. The density-matrix renormalization group in the age of matrix product states. *Annals of physics*, 326(1):96–192, 2011.
[96] Johannes Hauschild and Frank Pollmann. Efficient numerical simulations with tensor networks: Tensor network python (tenpy). *SciPost Physics Lecture Notes*, page 005, 2018.
[97] Nicola Marzari and David Vanderbilt. Maximally localized generalized wannier functions for composite energy bands. *Phys. Rev. B*, 56:12847–12865, Nov 1997.
[98] David Vanderbilt. *Berry phases in electronic structure theory: electric polarization, orbital magnetization and topological insulators*. Cambridge University Press, 2018.
[99] Xiao-Liang Qi. Generic wave-function description of fractional quantum anomalous hall states and fractional topological insulators. *Phys. Rev. Lett.*, 107:126803, Sep 2011.
[100] Daniel E. Parker, Xiangyu Cao, and Michael P. Zaletel. Local matrix product operators: Canonical form, compression, and control theory. *Phys. Rev. B*, 102:035147, Jul 2020.
[101] Tomohiro Soejima, Daniel E. Parker, Nick Bultinck, Johannes Hauschild, and Michael P. Zaletel. Efficient simulation of moiré materials using the density matrix renormalization group. *Phys. Rev. B*, 102:205111, Nov 2020.
[102] Frank Pollmann and Ari M Turner. Detection of symmetry-protected topological phases in one dimension. *Physical review b*, 86(12):125441, 2012.
[103] The in-principle possibility of a highly non-circular CFS outside of the LLL setting is therefore not realized here. We also do not observe significant *umklapp* scattering from higher Brillouin zones of composite Fermions.
[104] Junkai Dong, Jie Wang, and Liang Fu. Dirac electron under periodic magnetic field: Platform for fractional Chern insulator and generalized Wigner crystal. *arXiv e-prints*, page arXiv:2208.10516, August 2022.
[105] B. Estienne, N. Regnault, and V. Crépel. Ideal Chern bands are Landau levels in curved space. *arXiv e-prints*, page arXiv:2304.01251, April 2023.
[106] Jie Wang, Yunqin Zheng, Andrew J. Millis, and Jennifer Cano. Chiral approximation to twisted bilayer graphene: Exact intravalley inversion symmetry, nodal

structure, and implications for higher magic angles. *Phys. Rev. Research*, 3:023155, May 2021.

[107] J. K. Jain. Incompressible quantum hall states. *Phys. Rev. B*, 40:8079–8082, Oct 1989.

[108] X. G. Wen. Non-abelian statistics in the fractional quantum hall states. *Phys. Rev. Lett.*, 66:802–805, Feb 1991.

[109] Yuan-Ming Lu and Ying Ran. Symmetry-protected fractional Chern insulators and fractional topological insulators. *Physical Review B*, 85(16):165134, April 2012.

[110] John McGreevy, Brian Swingle, and Ky-Anh Tran. Wave functions for fractional Chern insulators. *Physical Review B*, 85(12):125105, March 2012.

[111] Ganpathy Murthy and R. Shankar. Composite Fermions for Fractionally Filled Chern Bands, September 2011.

[112] Ganpathy Murthy and R. Shankar. Hamiltonian theory of fractionally filled Chern bands. *Physical Review B*, 86(19):195146, November 2012.

[113] Maissam Barkeshli and John McGreevy. Continuous transitions between composite Fermi liquid and Landau Fermi liquid: A route to fractionalized Mott insulators. *Physical Review B*, 86(7):075136, August 2012.

[114] Maissam Barkeshli and John McGreevy. Continuous transition between fractional quantum Hall and superfluid states. *Physical Review B*, 89(23):235116, June 2014.

[115] E. Rezayi and N. Read. Fermi-liquid-like state in a half-filled Landau level. *Physical Review Letters*, 72(6):900–903, February 1994.

[116] Note that while continuous translation symmetry fixes $\psi^{\mathrm{CF}}_{\boldsymbol{k}}(\boldsymbol{r}) = e^{i\boldsymbol{k}\cdot\boldsymbol{r}}$ in the LLL, different Bloch states may be used for systems with lattice translation symmetry. Likewise, the composite Fermi surface need not be flat.

[117] Max A. Metlitski and Ashvin Vishwanath. Particle-vortex duality of two-dimensional dirac fermion from electric-magnetic duality of three-dimensional topological insulators. *Physical Review B*, 93(24), jun 2016.

[118] Chong Wang and T. Senthil. Composite fermi liquids in the lowest landau level. *Phys. Rev. B*, 94:245107, Dec 2016.

[119] Chong Wang and T. Senthil. Half-filled landau level, topological insulator surfaces, and three-dimensional quantum spin liquids. *Phys. Rev. B*, 93:085110, Feb 2016.

[120] Song He, P. M. Platzman, and B. I. Halperin. Tunneling into a two-dimensional electron system in a strong magnetic field. *Phys. Rev. Lett.*, 71:777–780, Aug 1993.

[121] Naoto Nagaosa, Jairo Sinova, Shigeki Onoda, A. H. MacDonald, and N. P. Ong. Anomalous hall effect. *Rev. Mod. Phys.*, 82:1539–1592, May 2010.

[122] Andrew C. Potter, Maksym Serbyn, and Ashvin Vishwanath. Thermoelectric transport signatures of dirac composite fermions in the half-filled landau level. *Physical Review X*, 6(3), aug 2016.

[123] Chong Wang, Nigel R. Cooper, Bertrand I. Halperin, and Ady Stern. Particle-hole symmetry in the fermion-chern-simons and dirac descriptions of a half-filled landau level. *Phys. Rev. X*, 7:031029, Aug 2017.

[124] Taige Wang, Trithep Devakul, Michael P. Zaletel, and Liang Fu. Topological magnets and magnons in twisted bilayer mote$_2$ and wse$_2$, 2023.

[125] Hart Goldman, Aidan P. Reddy, Nisarga Paul, and Liang Fu. Zero-field composite fermi liquid in twisted semiconductor bilayers, 2023.

[126] Yugo Onishi and Liang Fu. Quantum geometry, optical absorption and topological gap bound, 2023.

[127] Heonjoon Park, Jiaqi Cai, Eric Anderson, Yinong Zhang, Jiayi Zhu, Xiaoyu Liu, Chong Wang, William Holtzmann, Chaowei Hu, Zhaoyu Liu, Takashi Taniguchi, Kenji Watanabe, Jiun haw Chu, Ting Cao, Liang Fu, Wang Yao, Cui-Zu Chang, David Cobden, Di Xiao, and Xiaodong Xu. Observation of fractionally quantized anomalous hall effect, 2023.

[128] Daniel Parker, Patrick Ledwith, Eslam Khalaf, Tomohiro Soejima, Johannes Hauschild, Yonglong Xie, Andrew Pierce, Michael P. Zaletel, Amir Yacoby, and Ashvin Vishwanath. Field-tuned and zero-field fractional Chern insulators in magic angle graphene. *arXiv e-prints*, page arXiv:2112.13837, December 2021.

[129] Qiang Gao, Junkai Dong, Patrick Ledwith, Daniel Parker, and Eslam Khalaf. Untwisting moiré physics: Almost ideal bands and fractional chern insulators in periodically strained monolayer graphene, 2022.

[130] A. M. Läuchli, Zhao Liu, E. J. Bergholtz, and R. Moessner. Hierarchy of fractional chern insulators and competing compressible states. *Phys. Rev. Lett.*, 111:126802, Sep 2013.

[131] Zhao Liu and Emil J. Bergholtz. From fractional Chern insulators to Abelian and non-Abelian fractional quantum Hall states: Adiabatic continuity and orbital entanglement spectrum. *Physical Review B*, 87(3):035306, January 2013.

[132] Nick Bultinck, Eslam Khalaf, Shang Liu, Shubhayu Chatterjee, Ashvin Vishwanath, and Michael P. Zaletel. Ground state and hidden symmetry of magic-angle graphene at even integer filling. *Phys. Rev. X*, 10:031034, Aug 2020.

[133] Oskar Vafek and Jian Kang. Renormalization group study of hidden symmetry in twisted bilayer graphene with coulomb interactions. *Phys. Rev. Lett.*, 125:257602, Dec 2020.

[134] E. H. Rezayi and F. D. M. Haldane. Incompressible paired hall state, stripe order, and the composite fermion liquid phase in half-filled landau levels. *Phys. Rev. Lett.*, 84:4685–4688, May 2000.

[135] F. D. M. Haldane and E. H. Rezayi. Periodic laughlin-jastrow wave functions for the fractional quantized hall effect. *Phys. Rev. B*, 31:2529–2531, Feb 1985.

[136] F. D. M. Haldane. Many-particle translational symmetries of two-dimensional electrons at rational landau-level filling. *Phys. Rev. Lett.*, 55:2095–2098, Nov 1985.

[137] Jie Wang, Scott D. Geraedts, E. H. Rezayi, and F. D. M. Haldane. Lattice monte carlo for quantum hall states on a torus. *Phys. Rev. B*, 99:125123, Mar 2019.

[138] Junping Shao, Eun-Ah Kim, F. D. M. Haldane, and Edward H. Rezayi. Entanglement entropy of the $\nu = 1/2$ composite fermion non-fermi liquid state. *Phys. Rev. Lett.*, 114:206402, 2015.

[139] Jie Wang. Dirac fermion hierarchy of composite fermi liquids. *Phys. Rev. Lett.*, 122:257203, Jun 2019.

[140] F. D. M. Haldane. The origin of holomorphic states in landau levels from non-commutative geometry and a new formula for their overlaps on the torus. *Journal of Mathematical Physics*, 59(8):081901, 2018.

[141] F. D. M. Haldane. A modular-invariant modified weierstrass sigma-function as a building block for lowest-landau-level wavefunctions on the torus. *Journal of Mathematical Physics*, 59(7):071901, 2018.

[142] J. K. Jain and R. K. Kamilla. Quantitative study

of large composite-fermion systems. *Phys. Rev. B.*, 55:R4895(R), 1997.

[143] Songyang Pu, Ying-Hai Wu, and J. K. Jain. Composite fermions on a torus. *Phys. Rev. B*, 96:195302, Nov 2017.

[144] Daniel E. Parker, Tomohiro Soejima, Johannes Hauschild, Michael P. Zaletel, and Nick Bultinck. Strain-induced quantum phase transitions in magic-angle graphene. *Phys. Rev. Lett.*, 127:027601, Jul 2021.

[145] Tianle Wang, Daniel E Parker, Tomohiro Soejima, Johannes Hauschild, Sajant Anand, Nick Bultinck, and Michael P Zaletel. Kekul\'e spiral order in magic-angle graphene: a density matrix renormalization group study. *arXiv preprint arXiv:2211.02693*, 2022.

[146] Bogdan Pirvu, Valentin Murg, J Ignacio Cirac, and Frank Verstraete. Matrix product operator representations. *New Journal of Physics*, 12(2):025012, 2010.

[147] Dániel Varjas, Michael P Zaletel, and Joel E Moore. Chiral luttinger liquids and a generalized luttinger theorem in fractional quantum hall edges via finite-entanglement scaling. *Physical Review B*, 88(15):155314, 2013.

[148] Xue-Yang Song, Hart Goldman, and Liang Fu. Emergent qed_3 from half-filled flat chern bands, 2023.